

Equilibrium and off-equilibrium dynamics in a model for vortices in superconductors

Mario Nicodemi^{1,2,*} and Henrik Jeldtoft Jensen^{1,†}

¹*Department of Mathematics, Imperial College, 180 Queen's Gate, London SW7 2BZ, United Kingdom*

²*Università di Napoli "Federico II," Dip. Scienze Fisiche, INFN and INFN, Via Cintia, 80126 Napoli, Italy*

(Received 3 July 2001; published 1 April 2002)

We study a model for the dynamics of vortices in type-II superconductors. In particular, we discuss the magnetization relaxation close to and off equilibrium. At low temperatures a crossover point is found, T_g , where relaxation times become huge and seem to diverge according to a Vogel-Tamman-Fulcher law at a lower temperature T_c where a thermodynamic glass transition might be located. Magnetic creep changes by crossing T_g : below T_g , vortex motion is strongly subdiffusive and logarithmic creep is found; above T_g , a power-law creep is asymptotically followed by stretched exponential saturation. The analysis of the self-scattering function also reveals that the dynamical process is non-Gaussian. In the regime below T_g , strong “memory” and “aging” effects appear. In particular, we analyze the properties of “aging” and the structure of its “dynamical scaling.”

DOI: 10.1103/PhysRevB.65.144517

PACS number(s): 75.10.-b, 47.32.Cc, 74.60.Jg

I. INTRODUCTION

The nature of the dynamics of vortices in type-II superconductors has been discussed for many years, because of its important implications on system properties.¹⁻⁴ In particular, in the last few years it was discovered that many experiments are affected by strong dynamical off-equilibrium effects. Magnetization loops, magnetic creep, and current-voltage characteristics exhibit important, often even dominant, *history*-dependent features, such as “aging,” memory, and hysteresis (see Refs. 3–18 and references therein).

The existence of equilibrium “glassy” thermodynamic phases in vortex matter was suggested several years ago.^{1,18} In glass formers these phase transitions are called “ideal” glass transitions,¹⁹ because huge equilibration times often make such phases experimentally inaccessible. A glassy dynamics arises when the system intrinsic relaxation time becomes of the order of or longer than the time scale on which the system is probed. When this happens the system may not be able to reach thermodynamic equilibrium on any time scale allowed in experiments. Thus, to understand the observed phenomenology, we need to understand the relaxation of the system far from equilibrium, and, accordingly, to develop models of the relevant relaxation mechanisms in the vortex system.

In the present paper we focus on a model for *magnetic relaxation* in vortex matter.²⁰ In particular, we analyze the properties of “aging” observed in low-temperature creep,¹⁴ and its dynamical scaling structure. We elaborate on several details, especially concerning the dependence of relaxation times on temperature and external magnetic field. We will also outline similarities with ordinary glass formers such as polymers or supercooled liquids.^{19,21,22}

Magnetization is the simplest and most natural quantity to characterize the state of the vortex system. Interestingly, magnetization measures exhibit many important, markedly *out-of-equilibrium* features such as the presence of hysteretic cycles, the dependence on the sweep rate of the external field, logarithmic relaxation (suggesting the existence of huge relaxation times), “aging,”¹⁴ and other similar pro-

nounced “memory” and “metastability” effects (see the references cited in Refs. 3–11,16, and 23–25).

Under typical experimental conditions, the vortex density in the sample is high enough to produce a many-body system of strongly interacting “particles.” Thus, even “simplified” approaches to dynamical properties, such as the time-dependent Ginzburg-Landau theory, are extremely difficult to deal with from a technical point of view, and it is often necessary to introduce phenomenological approaches such as Kim-Anderson-like “macroscopic” descriptions.¹⁻⁴

It is in this perspective that we consider a simple schematic statistical mechanics lattice model to describe some common properties of vortex dynamics in type-II superconductors from a more “microscopic” point of view. Our model can be understood in the well-established theoretical framework of statistical mechanics of disordered media.²⁶ It is a phenomenological lattice Hamiltonian model for the effective vortices dynamics, studied with Monte Carlo (MC) simulations. Such a MC-driven model has been shown to reproduce a very broad range of experimental observations: in addition to a reentrant equilibrium phase diagram, the model reproduces dynamical phenomena such as slow creep dynamics, the hysteresis of magnetization loops, the “second peak” structure in magnetization loops, “memory” and irreversibility of I - V characteristics, and several others.²⁰ Hence the model seems to be able to give a unified and comprehensive description of magnetic and transport properties in vortex matter.

It is interesting that our MC dynamics shows a very good correspondence with this very diverse range of experiments on vortices. MC dynamics is known to be an efficient representation of dynamics of systems which contains slow diffusive degrees of freedom,²⁷ and it is well known that the general features of relaxation processes in glassy systems, such as supercooled liquids or spin glasses,^{26,28} are well represented by the MC method. Interestingly, our results are in agreement with those from over damped Langevin molecular-dynamics simulations of vortex systems,^{20,29} when available.

Our model, introduced mainly to study the dynamics, to

some extent captures some of the essential elements of the phase diagram. In correspondence with experiments (see for instance, references in Refs. 30–32) our numerical simulations show, for instance, several phase transitions at low temperatures when the applied magnetic field is increased: a couple of reentrant discontinuous transitions at very small and large fields and, between them, an other discontinuous transition associated to the location of the second magnetization peak (see Ref. 20).

The picture of creep which emerges from our model is schematically the following: at low temperatures T , the system free-energy landscape is characterized by the presence of *self-generated* very high barriers (of both entropic and energetic origin).²⁰ This implies that, on lowering T , the characteristic relaxation time enormously increases and eventually, at a crossover point, T_g , becomes longer than the time scale on which the observation of the system is made. In analogy with similar phenomena in glass-forming liquids, we call such a loosely defined crossover temperature T_g the “phenomenological glass transition temperature.”^{19,22} Around T_g , or whenever the experimental (or simulation) time scales are shorter than the equilibration times, strong off-equilibrium properties appear: “memory,” “aging,” dependence on external driving rates, and similar properties.

At intermediate temperatures, larger than T_g , we observe a nonexponential relaxation of the magnetization: a power-law decay is asymptotically followed by a stretched exponential behavior (the Kohlrausch-Williams-Watts law found in glass formers.¹⁹) Below T_g , the off-equilibrium relaxation follows a power law at very short times, and later is well approximated by the well-known logarithmic relaxation of thermally assisted flux flow.¹ In particular, we find the existence of “aging” with “dynamical scaling” of purely dynamical origin in off-equilibrium two-time correlation functions $C(t, t')$, a fact very important for understanding the nature of the relaxation of the vortex system, and which necessitates new basic experiments. This phenomenon corresponds to the known “aging” behaviors found in other glassy systems.²¹ The crossover temperature T_g is associated with a change in the properties of vortex motion at a microscopic level: diffusive above T_g ; below T_g it becomes strongly subdiffusive. The analysis of the self-scattering function $F_q(t, t')$ reveals, however, that also above T_g the system overall relaxation is a non-Gaussian process resembling those present in other complex fluids.¹⁹

At even lower temperatures a true thermodynamic “ideal glass transition” T_c may exist,¹ which we locate by a Vogel-Tamman-Fulcher fit of the relaxation time as a function of the temperature. What we stress here is that strong “glassy” features can appear even if $T_c=0$ (as expected in two-dimensional systems), whenever the system is below T_g .^{19–21}

Our model gives predictions on the structure of these phenomena, and their mutual relationships, describe the system’s *equilibrium* and *off-equilibrium* dynamics, and establish definite predictions, as for instance for the properties of its “aging.” The above scenario appears to be in very good correspondence with experiments about vortex creep in superconductors where, in particular, recent experimental re-

sults also pointed out that aging properties are actually found in magnetic creep,¹⁴ and crossover temperatures are well known to exist in vortex creep (see, for instance, Refs. 33 and 34 and references in Ref. 3).

The paper is organized in the following way. In Sec. II we describe the model. In Sec. III we discuss the relaxation of the magnetization and its characteristic time scales. In Sec. IV we discuss the two-time correlation functions of the magnetization, and identify the structure of aging and memory aspects of vortex dynamics. In Sec. V we turn to the spatial characterization of the vortex system in the glassy regime. For this purpose we consider self-diffusion and self-scattering functions. Finally Sec. VI contains our conclusions.

II. MODEL

In type-II superconductors an external magnetic field can penetrate into the sample, forming the well-known vortex lines. These generally repel each other and typically interact with a quenched disordered background, such as pinning sites, which exert short-ranged forces on vortices.² In many materials, the vortex-vortex, and vortex-pin interaction energy scales can be comparable to thermal fluctuations: the presence of these competing energies leads to a variety of important and surprising phenomena of vortex matter.^{1–4}

In the simple case of straight parallel vortex lines, it is well known that, away from the upper critical field, the vortex pair interaction potential is, usually, screened beyond the field penetration length λ . In particular, the potential has approximately an exponential decay at large intervortex distances (controlled by λ), and saturates at a finite maximum when the intervortex distances is of the order of the correlation length ξ (see, for instance, Ref. 2).

This technically means that interactions are short ranged in the sense used in field theory. However, in many compounds, for typical values of the magnetic field, λ can be much larger than the average vortices separation. In fact, by increasing the external field the vortex density grows, and the vortex average distance a_0 can become much smaller than λ . This implies that each vortex significantly interacts with very many other vortices. This fact cannot be ignored, and results in one of the essential difficulties theoretical approaches have to face: dealing with a highly interacting many-body system with several relevant length scales.

To cope with these difficulties, we consider a simplified model which is a schematic coarse-grained lattice version of a real interacting vortex system.²⁰ It is worth recalling that the coarse-graining technique used here is similar to other well-known coarse-graining approaches to multiscale problems ranging from magnetism to structural defects in crystal (see Ref. 35). The basic underlying idea is that, under certain conditions (often not easy to be formally established³⁵), the properties of a system with \mathcal{N} degrees of freedom can be described using a smaller set \mathcal{N}' , by disregarding phenomena occurring below the smallest scale of interest in the problem.

Our model is a coarse-grained version of a vortex system described by Ginzburg-Landau equations in the London approximation. We coarse grain the original system of vortices

on a given length scale l_0 . This produces a Hamiltonian lattice system whose coarse-grained interaction potential can be simpler than the original one. The coarse-graining length l_0 is a parameter that one can opportunely tune: if l_0 is very small, say smaller than ξ , our model coincides with the original Ginzburg-Landau one. Our approximation here is to take a finite coarse-graining length l_0 . Since l_0 can be larger than ξ (we take $l_0 \simeq \lambda$), each coarse-grained lattice site can be multiply occupied. The occupancy is, however, restricted by the upper critical field B_{c2} . For this reason, we call the model a restricted occupancy model (ROM).²⁰

The model aims to find a compromise between the complexity of real physical interactions and the crucial advantage of having a system with a simplified interaction matrix which is analytically and numerically tractable in both its equilibrium and dynamical aspects. Of course, an intrinsic limitation appears: one cannot have information about system properties on scales smaller than l_0 . In the present case, however, our main interest is to explore the system dynamics, with particular reference to the region at low temperatures and high vortex densities where “glassy” features substantially appear, characterized by long time and space scales (much larger than λ). In such a region we expect that the finite l_0 approximations is not too drastic, and the fact that we reproduce many of the known experimental observations on magnetic relaxation may be an indication for that. Many important models of vortex dynamics, such as the Kim-Anderson model (which is a mesoscopic model, i.e., a model coarse grained on a scale much larger of the one we adopt here), are unable to describe the equilibrium phases of the system. Interestingly enough, the present model also captures some of the essential elements of the phase diagram.²⁰

Coarse graining of the vortex system at zero temperature has been used in the past, as, for instance, in Refs. 36–38. At variance with these coarse-grained cellular automata, the ROM is a full statistical mechanics model which explicitly considers the fact that the vortex system is in contact with a thermal bath and has a finite value of B_{c2} . Another important difference consists in our use of a standard MC Kawasaki dynamics²⁷ to model the system relaxation and not deterministic cellular automata rules. We will see that all these facts are of crucial relevance to understand the system properties.

A. Hamiltonian

In order to consider only the fundamental interactions in the system, we ignore other important but more specific effects such as surface barriers, and consider just the above-cited three energy scales: vortices repulsion, vortex-pin coupling, and thermal fluctuations. A system of straight parallel vortex lines, corresponding to a magnetic field B along the z axis, interacts via a potential²

$$A(r) = \frac{\phi_0^2}{2\pi\lambda'^2} [K_0(r/\lambda') - K_0(r/\xi')], \quad (1)$$

where

$$\xi' = c\xi/\sqrt{2} \quad \text{and} \quad \lambda' = c\lambda, \quad c = (1 - B/B_{c2})^{-1/2}. \quad (2)$$

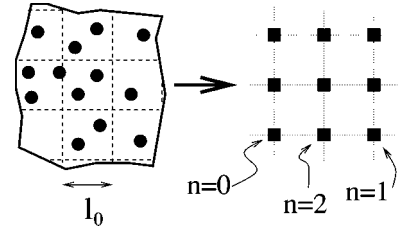


FIG. 1. A schematic diagram of the coarse-grained model dealt with in the present paper. The original vortex system (left) is coarse grained on a length scale l_0 , and mapped into a lattice model where multioccupancy is allowed (ROM is the reduced occupancy model).

Here K_0 is the MacDonal function, and ξ and λ are the correlation and penetration lengths. The coarse graining of the original vortex system in the xy plane is made by introducing a square grid of lattice spacing, l_0 , of the order of the London length, λ (see Fig. 1). By this procedure, the original vortex system is mapped into a lattice model characterized by a classical field n_i . The coarse-grained model Hamiltonian has the following form:

$$\mathcal{H} = \frac{1}{2} \sum_{ij} n_i A_{ij} n_j - \frac{1}{2} \sum_i A_{ii} |n_i| - \sum_i A_i^p |n_i|. \quad (3)$$

Since a lattice site is a coarse-grained representation of a surface of area of order l_0^2 in the original system, the occupancy of lattice sites in Eq. (3) is an integer variable equal to the net number of particles on site i , $n_i \in \{-N_{c2}, \dots, -1, 0, 1, \dots, N_{c2}\}$ (see Fig. 1). The parameter N_{c2} (Ref. 39) bounds the particle density per site below a critical value, and is schematically related to the upper critical field B_{c2} characteristic of type-II superconductors (see below). Particles on each site have an overall “charge” (associated with the two possible orientations of magnetic flux) and neighboring particles with opposite “charge” can annihilate (or be created, which generally implies an high energy cost).

The first term in Eq. (3) represents the repulsion between the particles.² In the limit of small l_0 (say, $l_0 \leq \xi$), the coarse-grained potential A_{ii} coincides with the “full” interaction $A(r)$ obtained in the London limit from Ginzburg-Landau theory. The ROM thus corresponds to standard models already studied. The problem with the models obtained in such a small l_0 limit is that they are hardly feasible to explore the region of long time and space scales at low temperatures and high magnetic fields where “glassy” features substantially appear. On the contrary, for l_0 of the order of λ (the value used here), the ROM is suited to describe the above “complex” fluid or glassy behaviors of vortex matter, but does not catch its features at shorter length scales.

As already stated, here we take the coarse graining length l_0 of order the of the range of interaction between the vortices, and thus consider a finite range potential A_{ij} . We assume $A_{ii} = A_0 = 1$: $A_{ij} = A_1$ if i and j are nearest neighbors, and $A_{ij} = 0$ for all others pairs of sites.³⁹ The effective range of the vortex-vortex interaction, λ' and ξ' in Eq. (1), depends on the temperature and magnetic field, thus the ratio between the coarse-graining length l_0 and λ' will change with temperature and magnetic induction. This implies that if

l_0 is fixed, one should let A_{ij} change with T and B . In particular, it would be more realistic to include off-diagonal terms in A_{ij} beyond nearest-neighbor interactions when λ' begins to become large compared with l_0 . At present we neglect these complications, and use only the simple nearest-neighbor form of A_{ij} described above, but this does not affect the general results we find. As will become clear below, this T - and B -independent form of A_{ij} is sufficient to describe many features of the vortex system.

The second term in Eq. (3) concerns the particle self-interaction energy: in brief, it imposes that a single vortex left alone has no “interaction energy.” The third term corresponds to a random pinning potential, with a given distribution $P(A^p)$, acting on a fraction p of lattice sites (typically below we use $p=1/2$). For simplicity we choose a delta-distributed random pinning: $P(A^p) = (1-p)\delta(A^p) + p\delta(A^p - A_0^p)$.³⁹

To control the overall system “charge density,” one can add a chemical potential term $-\mu\sum_i n_i$ to the above Hamiltonian, and study the system in the grand canonical ensemble, a fact which proves to be useful in analytical approaches.²⁰

B. Parameters of \mathcal{H}

The parameters entering the model can be qualitatively related to material parameters of superconductors. We can relate the coarse-graining length l_0 to the upper critical field B_{c2} through the relation $N_{c2}\Phi_0 \propto B_{c2}l_0^2$, where $\Phi_0 = hc/2e$ is the unit quantum magnetic flux. This implies

$$l_0 \propto N_{c2}^{1/2} \xi. \quad (4)$$

Thus we have related the coarse graining length scale l_0 , the superconducting coherence length ξ and the ROM is upper occupancy bound N_{c2} .

The energy scale unit in the model is set by the intervortex coupling A_0 , to which all the other energy scales, such as A_1 and A^p , have to be compared. The ratio $\kappa^* = A_1/A_0$ can be related to the Ginzburg-Landau parameter $\kappa = \lambda/\xi$ and, in typical cases, is expected to be an increasing function of κ . Asymptotically, vortex line segments interaction is exponential $A(r) \sim V_0 \exp(-r/\sqrt{2}\lambda)$.² Then, since by definition l_0 is the coarse-grained lattice spacing length, when l_0 is sufficiently large one can approximately write $A_0/A_1 \sim A(0)/A(l_0)$. For $l_0 \approx \lambda$, this in turn implies that

$$\ln \frac{1}{\kappa^*} \sim \sqrt{\frac{N_{c2}}{2}} \frac{1}{\kappa}. \quad (5)$$

Finally, the average pinning strength A_0^p is assumed to be a reasonable fraction, α_p (below $\alpha_p=0.3$), of A_0 :

$$A_0^p = \alpha_p A_0. \quad (6)$$

The temperature scale of the ROM can be directly related to the physical temperature of the vortex system in a superconductor. The most meaningful way of doing this is to compare the structure of the equilibrium phase diagram of the

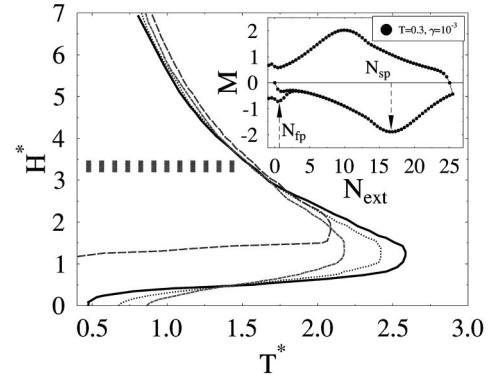


FIG. 2. Main frame: the phase diagram of the ROM in the plane (H^*, T^*) , where $H^* = \mu/k_B T$ and $T^* = T/A_1$ are the dimensionless chemical potentials of the external applied field and temperature. It is evaluated in mean field approximation in the small pinning strength regime ($A_0^p < A_0$), for $\kappa^* = 10$ and $A_0^p = 0.0, 0.5$, and 0.75 (full, dotted, and dashed lines) and $\kappa^* = 3.3$ and $A_0^p = 0.0$ (long dashed line). Computer simulations of the ROM in two dimensions, at low T by increasing the field, also reveal a couple of first-order reentrant phase transitions and, between them, another first-order transition associated with the second magnetization peak, which here is schematically shown by the broad horizontal dashed line. Inset: hysteresis magnetization loop with an “anomalous” second peak, $N_{sp}(\gamma)$. The magnetization M is plotted as a function of the applied field density, N_{ext} , in the ROM during a cycling of the field, for $\kappa^* = 0.26$ at $T = 0.3$, and for a sweep rate $\gamma = 10^{-3}$.

ROM to the corresponding phase diagram of the vortex system (see Fig. 2, the discussion below, and Ref. 20).

C. Model dynamics

On a macroscopic scale, the equations describing the state of the vortices are the Maxwell equations combined with the material equation associated with the electromagnetic response of a superconductor, which in turn depends on the dynamics of vortices. This is the basis for the classic thermally assisted flux flow theory.¹⁻⁴ From a more microscopic point of view, vortex motion has been described by time-dependent Ginzburg-Landau equations and typically, in the London limit, by considering as essential degrees of freedom only the vortex positions. Simulations have often assumed that the vortex dynamics could be modeled by a set of overdamped Langevin molecular-dynamics equations for the vortex positions,^{29,40-42} but even in this limit it is hardly possible to explore the long time and space scales, and the high-density region physics where glassy features essentially appear.

It is an experimental observation that diffusion modes are very important in vortex systems: vortices undergo a sort of “Brownian” motion in their wandering in the sample,^{43,44} as also found in molecular dynamics.⁴⁵ With this in mind we assume that the vortex dynamics is a stochastic diffusion process in a thermal bath, in the presence of conservative interaction potentials describing the vortex-vortex and vortex-pinning interactions, as summarized in the Hamiltonian equation (3). The simplest consistent approach for simulating the system relaxation at nonzero temperatures

consists in a Monte Carlo Kawasaki dynamics²⁷ (here on a square lattice of size L) at a temperature T (see Ref. 39) This is a standard approach in computer simulations of dynamical processes in complex fluids.²⁷ We allow vortex-antivortex annihilation and creation on neighboring sites. In particular, we suppose that the system is in contact with an external reservoir of “particles” through surfaces of the system. This external reservoir schematically corresponds to the applied field present in magnetic experiments on superconductors. Particles are introduced and escape the system only through the reservoir, which, by definition, has a given density N_{ext} . In the absence of pinning and other forces, the internal *equilibrium* density N_{in} satisfies $N_{ext}=N_{in}$. However, as we shall see below, this is an ideal case which will change dramatically in the presence of pinning (see the Bean profiles in Fig. 9).

D. Numerical simulations

In what follows we typically consider a two-dimensional square lattice which is periodic in one direction and has the other two edges coupled to the external reservoir (i.e., a cylinder geometry). We performed MC simulations on lattices of linear size $L=32$ (but we checked our results in the size range $L \in \{8, \dots, 128\}$) described by Eq. (3) (where the parameters are usually $A_0=1.0$, $A_0^p=0.3$, and $N_{c2}=27$) in the presence of a thermal bath at temperature T . We have sampled several values of $\kappa^* \equiv A_1/A_0 \in [0, 0.3]$. Our numerical statistical averages run, according to system size, from 128 to 1024 thermal noise and pinning realizations.

The ROM is able to describe a large variety of dynamical properties observed in type-II superconductors.²⁰ Here we focus on the dynamical properties of the system in the low- T region. This is the region where mean-field theory shows that the equilibrium phase diagram of the model (shown in Fig. 2) in the applied field-temperature plane has a reentrant phase transition line from a high-temperature, low-density fluid phase to an ordered phase,²⁰ in analogy to predictions^{1,46} and observations (see for instance references in Refs. 30 and 32) in superconductors. In good comparison with experiments (see references in Refs. 30 and 32) also our numerical simulations for finite dimensional systems (i.e., non-mean-field) show a sequence of phase transitions: for instance, when the field is increased two reentrant discontinuous transitions are found (as much as in mean-field theory) and, between them, another discontinuous transition associated to with the location of the second magnetization peak (this is described in more detail in Ref. 20).

In our numerical simulations below, we usually keep the temperature T fixed and ramp the “external field” N_{ext} (starting from zero up to some given value) at a given sweep rate γ : $\gamma = \Delta N_0 / \tau_{ext}$, where τ_{ext} is the time we spend at a each value of N_{ext} and ΔN_0 is its step increment during the ramp.

III. MAGNETIZATION RELAXATION

A very natural and important quantity which characterizes the state of the system is the magnetization $M(t)$,

$$M(t) = N_{in}(t) - N_{ext}(t), \quad (7)$$

where $N_{in} = \sum_i n_i / L^2$ is the total “charge” density inside the system at time t , and N_{ext} is the applied field. As in typical experiments, we record the isothermal magnetization $M(t)$. Time is measured in such a way that unity corresponds on average to a full Monte Carlo sweep of the lattice.

First we briefly consider magnetization loops: the applied field N_{ext} is ramped at a given “sweep rate” γ , up to a given value, and then decreased back to zero. We typically find hysteretic magnetization loops with shapes that closely resemble experimental observations^{23–25,30,32,47} (for details see Ref. 20). In particular, when κ^* is above a critical value $\kappa_c^* \approx 0.25$ (which is the regime we consider below), a pronounced second peak is observed in M , as shown in Fig. 2, which was shown to correspond to a first-order phase transition.²⁰

In what follows, we are interested in studying the properties of magnetic relaxation (i.e., creep) when, during these magnetization loops, the external field is at some point fixed at a given working value N_{ext} , and the vortex system is allowed to isothermally evolve.

A. Relaxation above T_g

The thermal creep of vortices significantly depends, as explained below in detail, on the value of the applied field N_{ext} , on the temperature T , and on the field sweep rate γ (and on system interactions parameters κ^* , A^p , and size L).

In particular, the nature of the dynamics change qualitatively by decreasing T . For the sake of clarity, we first consider the creep dynamics at relatively “high” temperatures where it is possible to investigate the dynamics of the system *close to equilibrium*. We will also show that, in these “simple” situations, the relaxation has a nontrivial structure. At lower temperatures, below a certain crossover value T_g to be defined later, the nature of the dynamics qualitatively changes: for $T \leq T_g$ the system is typically well off equilibrium because the observation time scales are much shorter than the characteristic equilibration times. In this region one finds a “logarithmic” creep, corresponding to a subdiffusive motion of single vortices.

In what follows we consider a system which is zero-field-cooled at a given temperature T . We then ramp the external field (at a rate $\gamma = 10^{-3}$) up to the working value N_{ext} , and then we monitor the magnetic relaxation $M(t)$. Let us consider first the intermediate temperatures range where the system is close to equilibrium. As a typical case, we report the behavior of $M(t)$ at $T=1.0$ for a system characterized by an interaction parameter $\kappa^* = 0.28$. At that given temperature, we record the system evolution for several values of N_{ext} .

In the present regime, it is possible at long times to observe the saturation of $M(t)$ to its equilibrium value. The asymptotic long times decay is *not* exponential (see Fig. 3), but approximated by the so-called Kohlrausch-Williams-Watts (KWW) law (i.e., a stretched exponential),

$$M(t) - M(0) = \Delta M [1 - e^{-(t/\tau_M)^{\beta_M}}], \quad (8)$$

where $M(0)$ is the magnetization value when the applied field was set to the fixed working value N_{ext} (i.e., at $t=0$).

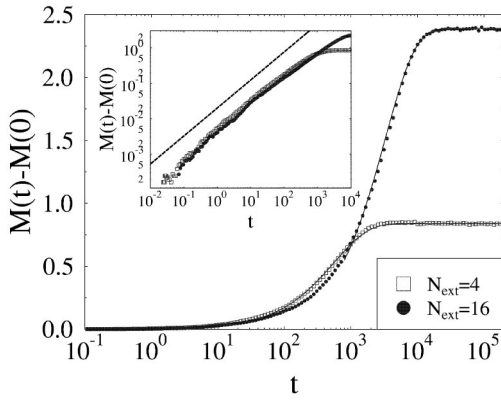


FIG. 3. Isothermal magnetization relaxation in the ROM for $\kappa^* = 0.28$ at $T = 1.0$, for the shown values of the external field N_{ext} (ramped from zero with a rate $\gamma = 10^{-3}$). Asymptotically, $M(t)$ is well fitted by the so-called Kohlrausch-Williams-Watts (KWW) law, i.e., stretched exponentials (continuous lines), but (see the inset) at short times a power-law relaxation is observed (the dashed line in the inset is to guide the eye).

The KWW relaxation is also typically found in glass formers above the glass transition.¹⁹ The time scale τ_M and the Kohlrausch exponent β_M (and the fit parameter ΔM) depend on the temperature T and on the overall field N_{ext} as shown in Figs. 4, 5, and 6. In particular, for a given N_{ext} , β_M increases with T and seems to approach a value of 1 when $T \rightarrow \infty$ (see Fig. 6). Figure 4 outlines, instead, the nonmonotonic behavior of τ_M with N_{ext} : τ_M has a broad maximum in correspondence with the location of the second magnetization peak, N_{sp} (see the inset of Fig. 2). The behavior of τ_M as a function of T and N_{ext} is a very important feature of great importance to the off-equilibrium behavior found in superconducting samples. Its effects can be seen, for instance, in the experimental observation of field dependent creep rates and magnetic loops.⁴⁸ In fact, in experiments (or computer

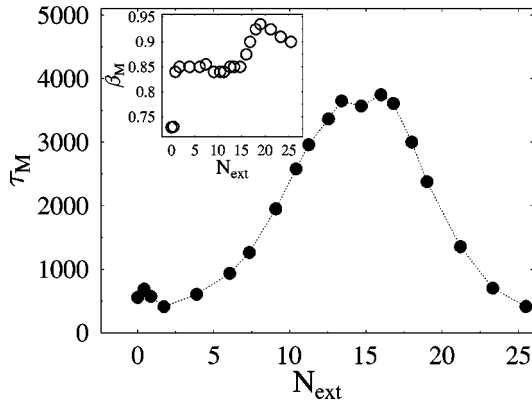


FIG. 4. The parameters of the Kohlrausch-Williams-Watts asymptotic magnetic relaxation shown in Fig. 3 ($T = 1.0$). Inset: the exponent β_M as a function of the applied field N_{ext} . Main panel: the equilibration time τ_M . Notice that τ_M is a non monotonous function of N_{ext} which spans about one decade. The location of the maximum of τ_M corresponds to the position of the “second peak” observed in magnetization loops (see Fig. 2). The first peak in τ_M is related to the crossing of the low field order-disorder transition.

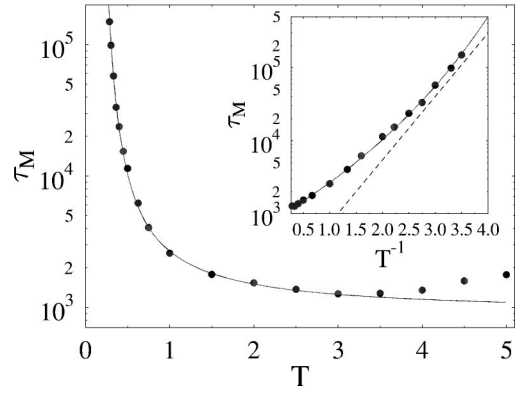


FIG. 5. The parameters of the Kohlrausch-Williams-Watts asymptotic relaxation of the magnetization as a function of the temperature T , recorded at $N_{ext} = 10$ after ramping the field with a rate γ as in Fig. 3. The equilibration time τ_M enormously grows by decreasing the temperature T . Below the crossover temperature $T_g \sim 0.25$, the system relaxation times are larger than the observation time. The Vogel-Tamman-Fulcher (VTF) fit of Eq. (10) is the superimposed curve. Inset: In the region where τ_M seems to diverge, we plot it as a function of $1/T$, and show the VTF fit of Eq. (10). For comparison also an Arrhenius curve is shown (dashed straight line).

simulations) the external field is typically ramped at a given rate γ , but whenever $\gamma \gg \tau_M^{-1}$ the system is taken out of equilibrium, simply because it is unable to follow the drive. Then “memory” and “aging” effects, along with dependences on the sweep rate, are immediate consequences. Actually, we can clearly see those effects in our system whenever we cool it too rapidly in the low- T regime, as discussed below.

The KWW relaxation characterizes the long-time regime of the vortex dynamics, which is analogous to the so-called α relaxation in supercooled liquids and glass formers.¹⁹ The asymptotic regime is markedly different from the short-time relaxation, the so-called β relaxation of supercooled liquids, where a power-law behavior is found (see the inset of Fig. 3):

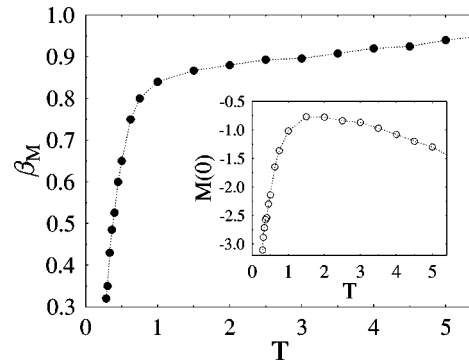


FIG. 6. The parameters of the Kohlrausch-Williams-Watts asymptotic relaxation of the isothermal magnetization as a function of the temperature T , recorded at $N_{ext} = 10$ (the field was ramped from zero with a rate γ as in Fig. 3). By lowering T , the exponent β_M decreases well below 1 (the value corresponding to a simple exponential relaxation). Inset: the value of the magnetization at the initial time $t = 0$ after the ramp has arrived at $N_{ext} = 10$.

$$M(t) - M(0) = M_0 \left(\frac{t}{\tau_M} \right)^{a_M}. \quad (9)$$

Even at the relatively high temperature $T=1.0$ (cf. Fig. 2), this power law holds for several orders of magnitude in time. We can numerically clearly distinguish the value of the exponent $a_M \approx 0.8$ (almost independent of N_{ext}) from β_M (a_M decreases from 1 at high T to $a_M \approx 0.8$ at $T=1.0$, and then remains almost constant with T). This shows that the dynamics is characterized by regions with different structures, and that the long-time relaxation is qualitatively different from the short time one. The KWW regime (which, for example, at $N_{ext}=16.8$ is found for $t > 10^3$; see Fig. 3) and the power-law regime (for $N_{ext}=16.8$ found when $t < 10^2$) are separated by an interesting crossover region whose duration increases with decreasing temperature (i.e., increasing equilibration time of the system), while the extension of power-law region shrinks.

It is important to mention that the above general results are not changed when the size of the system L is varied. However, as expected, increasing the system size does shift the characteristic time of relaxation: for example, at $T=1$ for $N_{ext}=10$ we find $\tau_M \propto L^2$ in the interval we spanned ($L \in [8, 128]$). This finding may be of importance to practical applications, since this implies that samples of different sizes may have very different equilibration and response times to external drive.

Another quantity which significantly affects τ_M is the interaction parameter κ^* . We have not investigated this in full detail, but we observe that a small increase of κ^* may result in a strong increase of τ_M .²⁰ Hence, for real superconductors, we expect a strong dependence of the characteristic time of magnetic relaxation on the Ginzburg-Landau parameter. Finally, as expected, τ_M increases with the amplitude of pinning energy, A^p .

B. Crossover temperature T_g

The scenario described above for $T=1.0$ is found in all regions of not too low temperature, but at lower T the picture changes. We plot τ_M and β_M as a function of T for $N_{ext}=10$ in Figs. 5 and 6 (similar results are found for different N_{ext}). It is very important to note that, around $T=0.5$, β_M drastically decreases and, at the same time, a steep increase of τ_M is found. In fact, for temperatures below $T_g \approx 0.25$, the characteristic relaxation time of the system (i.e., τ_M) becomes longer than our observation window. Consequently, below $T_g(N_{ext})$, the system is in an off-equilibrium state during our observation, and, as shown in detail below, typical glassy phenomena, such as ‘‘aging,’’ are observed. The crossover temperature T_g is itself a function of γ . It has a physical meaning similar to the so-called phenomenological glass transition point in supercooled liquids.¹⁹ Exploiting this analogy we will call this temperature the glass temperature despite the fact that in glassy systems it is only loosely defined.¹⁹ The existence of an underlying (lower) ‘‘ideal’’ glass transition point, T_c , is a subtle possibility which, in many cases (as supercooled liquids) still remain unresolved.

T_c is often located by extrapolation on τ_M data from the high T region, as we explain below.

The behavior of τ_M with the temperature gives important information about the system equilibration time scales (see Fig. 5). By decreasing the temperature, τ_M goes smoothly through a *minimum*, which, for $N_{ext}=10$, is around $T \approx 3.25$. As T is further decreased, τ_M strongly increases. The divergence at low temperatures can be fitted with a power law $\tau_M \sim (T - T_c)^{-\gamma}$, which gives $T_c \approx 0.21$ and $\gamma \approx 2.0$. However, for our data, a slightly better quality fit is found with the exponential Vogel-Tamman-Fulcher law (see the inset of Fig. 5),

$$\tau_M = \tau_0 \exp\left(\frac{E_0}{T - T_c}\right), \quad (10)$$

where, at $N_{ext}=10$, the characteristic time τ_0 is very large, $\tau_0 = 8.9 \times 10^2$, and the characteristic activation energy E_0 is ten times larger than T_c : $E_0 = 1.0$ and $T_c = 0.1$. The presence of a strong increase of τ_M close to a power law or a Vogel-Tamman-Fulcher law is again an example of the similarity with glassy features of supercooled liquids and glass formers.¹⁹ The above fits define the location of the ‘‘ideal’’ transition T_c . In the present case, they give a finite T_c , but, as much as in glasses, a standard Arrhenius fit [i.e., with Eq. (10), where $T_c = 0$] might also be consistent at very low T . In fact, since the present system is a two-dimensional system we expect that $T_c = 0$, but a finite T_c produces a better quality fit in all the data set of the range considered. Consistently with the present scenario, a Vogel-Tamman-Fulcher law has been also found in recent Molecular Dynamics simulations,²⁹ and was previously experimentally observed in Ref. 49.

Summarizing, we showed that about a certain crossover temperature $T_g(N_{ext})$ the characteristic relaxation time $\tau_M(N_{ext}, T)$ increases very rapidly with T , and as a consequence is bound to become larger than the observation time. In analogy with glass formers, T_g can be defined as the ‘‘phenomenological glass transition temperature.’’ By extrapolating the growth of τ_M with decreasing T , an ‘‘ideal glass transition’’ $T_c(N_{ext})$ can also be located. In the present case, where the pinning amplitude, A_p , is small, the value of T_c is not inconsistent with $T_c = 0$, as expected for a two-dimensional model, though from the simulation data we cannot rule out a $T_c > 0$.

C. Relaxation below T_g

Since below T_g relaxation times are huge, one might expect that the motion of the particles essentially freezes, apart from their vibration inside cages of other vortices. Instead, as we now shown, the off-equilibrium dynamics has remarkably rich properties.

In a narrow temperature interval around T_g the magnetization relaxation undergoes an important change. Actually, around and below T_g , $M(t)$ (see Fig. 7) has an initial power-law behavior as discussed above, but in the long-time region a logarithmic fit is definitely better than a stretched exponential with a very small exponent (say $\beta < 0.3$). A particularly

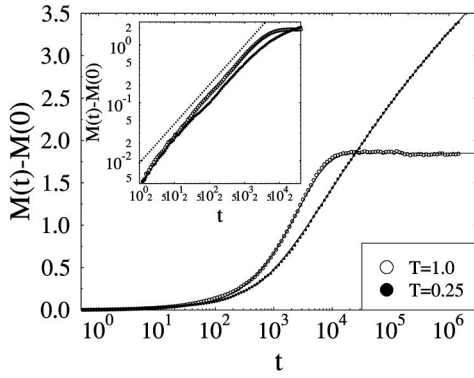


FIG. 7. The magnetization in the ROM at low temperatures shows a logarithmic creep. Here we plot data for $N_{ext}=10$ (after a ramp from $N_{ext}=0$ at a rate $\gamma=10^{-3}$) at the shown temperatures (for $\kappa^*=0.28$). Asymptotically, over at least four orders of magnitude in time, at $T=0.25$ $M(t)$ is well fitted by the usual logarithmic interpolation formula (continuous lines), but (see the inset) at very short times a power-law relaxation is still observed on a couple of decades (dashed line). For comparison we also plot the KWW stretched exponential relaxation found at $T=1.0$ (empty circles).

good fit is found by use of the well-known interpolation formula often used to describe vortex creep in experiments,¹

$$M(t) - M(0) \approx \Delta M_\infty \left\{ 1 - \left[1 + \frac{\mu T}{U_c} \ln \left(\frac{t + t_0}{t_0} \right) \right]^{-1/\mu} \right\}, \quad (11)$$

where $\mu \approx 1$ is consistent with our data. The above fit parameters are shown in Fig. 8 as a function of N_{ext} for $T=0.1$ (similar results are obtained for lower T). In agreement with previous findings, t_0 is a nonmonotonic function of N_{ext} . Interestingly, t_0 and $\mu T/U_c$ are linearly related, but, contrary to expectations from equilibrium considerations, U_c increases when t_0 decreases. This outlines that the value of U_c cannot be related to some characteristic “equilibrium energy barrier value,” which instead must increase with the equilibrium times scales as shown before.

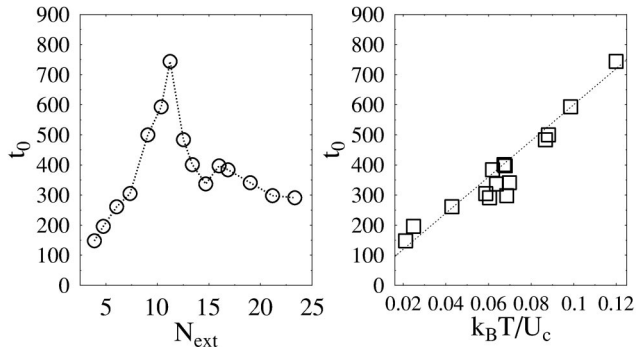


FIG. 8. The parameters of the asymptotic magnetization logarithmic creep as a function of N_{ext} , recorded at $T=0.1$ (the field was ramped from zero with a rate $\gamma=10^{-3}$). The “effective” barriers U_c and t_0 are strongly correlated: t_0 is smaller the larger U_c is (see the text).

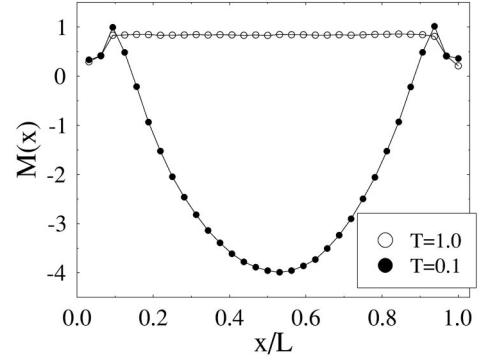


FIG. 9. The Bean profile of the local internal field, $M(x)$, as a function of the transversal coordinate x/L in a system of linear size $L=32$, for $N_{ext}=10$ at $T=1$ and 0.1 . The profiles are recorded after ramping the field (as in Fig. 7), and waiting up to $t=1.5 \times 10^6$ (i.e., up to the last point in Fig. 7).

The radically different states approached after the same relaxation time by the system at two different temperatures above and below T_g can be illustrated in the following way. In Fig. 9 we show the density profiles (i.e., the Bean profiles) of such two states. We measured the magnetization as a function of the sample transverse spatial coordinate, $M(x)$, at the end of our observation time window $t=1.5 \times 10^6$, for a system at $T=1.0$ (which is approximately at equilibrium) and another at $T=0.1$ (which, up to the recorded times, is off equilibrium). The system at $T=1.0$ has a flat density profile with no macroscopic heterogeneities; in contrast, the one at $T=0.1$ shows a pronounced Bean-like profile with strong spatial variations. The fact that close to the surface in the Bean profile we find a peak in M (i.e., $N_{in} > N_{ext}$) is again similar to experimental data (see, for instance, Ref. 6).

The good correspondence between the behavior of the ROM and a large amount of experimental works^{3,5–11,16,23–25,33,34,50–54} seems to confirm the schematic scenario for magnetic creep discussed here. It is also important to note that the above dynamical phenomena, ranging from slow relaxation or hysteresis to an anomalous “second peak” in magnetization loops, are found in very many different types of superconductors with a broad range of material parameters.^{5–11,16,23–25} This corroborate the hypothesis that a basic general (sample independent) mechanism is responsible for the observed complex phenomenology.

The famous Anderson-Kim model for magnetic relaxation in superconductors predicts the well-known logarithmic creep (asymptotically followed by an exponential).^{1–4} In “conventional” superconductors, such a behavior is typically found experimentally.³ However, in nonconventional superconductors the scenario is much more involved,³ the explanation of deviations from the Kim-Anderson model being one of the goals of collective flux-pinning models.¹ It has long been known that in YBCO crystals magnetic relaxation deviates from the Anderson-Kim prediction, and is better described by the collective pinning interpolation formula of Eq. (11) (see for instance, Ref. 50 and references in Ref. 3). Many other examples are well known,³ even in “unusual” materials. For instance in the organic superconductor $(\text{BEDT-TTF})_2\text{Cu}(\text{NCS})_2$, it is known that relaxation is loga-

rhythmic only below 1 K, whereas between 1.5 and 8 K power-law behavior is found.⁵¹ Power laws were also found in $\text{LuBa}_2\text{Cu}_3\text{O}_7$,⁵² in BSCCO (see, for instance, Ref. 23). A transition from low-temperature logarithmic to higher temperature power law was reported in both BSCCO (Ref. 33) and YBCO crystals^{53,54} (for a complete list of references, see Ref. 3 and also Refs. 5–11,16,23–25,30, and 32. Finally, a definite asymptotic crossover to a stretched exponential behavior is recorded in heavy fermion superconductors such as UPt_3 and UBe_{13} .⁵⁴ All these disparate observations can be reconciled in the present scenario.

IV. TWO-TIME CORRELATION FUNCTIONS

Above we discussed how sweep-rate-dependent hysteretic cycles, slowly relaxing magnetization, etc. indicate that our system, on the observed time scales, at low temperature is far from equilibrium. Actually, we have seen that by decreasing the temperature the dynamics slows down and that there exist a finite temperature below which the system cannot be equilibrated anymore within the time scale of the experiment or the computer simulation.

The appropriate tools to describe off-equilibrium behaviors, such as “aging” and “memory,” are two-time correlation functions because they clearly reveal the underlying nonstationarity of the dynamics.²¹ Thus in the simulations we described above, along with the magnetization $M(t)$, we also recorded the density-density correlation ($t > t_w$):

$$C(t, t_w) = \langle [N_{in}(t) - N_{in}(t_w)]^2 \rangle = \langle [M(t) - M(t_w)]^2 \rangle. \quad (12)$$

In fact, the analysis of $C(t, t_w)$ gives us access to more relevant information on the structure of the off-equilibrium dynamics than that contained in $M(t)$, as we discuss below.

A. Equilibrium relaxation

We have seen that at not too low temperatures, for instance at $T=1.0$, the system relaxation is characterized by finite relaxation times, but the dynamics is already nontrivial. The two-time correlator $C(t, t_w)$ is plotted in Fig. 10 for a relaxation at $N_{ext}=16.8$ after a ramp (from zero external field) with $\gamma=10^{-3}$ at $T=1.0$ (for a system with $\kappa^*=0.28$).

In agreement with the scenario recorded for $M(t)$, at long times, $C(t, t_w)$ is well fitted by the KWW stretched exponential form (see Fig. 10):

$$C(t, t_w) \simeq C_\infty [1 - e^{-[(t-t_w)/\tau]^\beta}]. \quad (13)$$

The exponent $\beta \simeq 1.4$ is almost constant for intermediate fields (see Fig. 11), but some weak variation could be spotted as function of N_{ext} . The characteristic time $\tau(N_{ext})$ has a nonmonotonic behavior with N_{ext} , shown in Fig. 11, and also its dependence on T is analogous to that found for τ_M .

At $T=1.0$, the two-time correlation function $C(t, t_w)$ shows no sign of “aging”: as expected for relaxations close to equilibrium, $C(t, t_w)$ is a function only of the time difference $t-t_w$ (up to the longest waiting time t_w , we probed, $t_w \in [10^2, 10^4]$). This is clearly seen in Fig. 12, where we plot

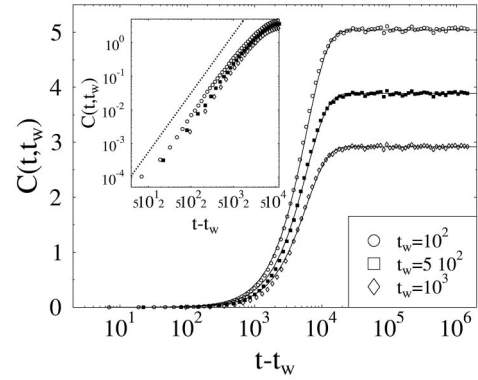


FIG. 10. The two time magnetization correlation function $C(t, t_w) = \langle [M(t) - M(t_w)]^2 \rangle$, plotted as a function of $t - t_w$, for $N_{ext}=10$ (after a ramp from $N_{ext}=0$ at a rate $\gamma=10^{-3}$) and $T=1$ ($\kappa^*=0.28$). At long times, over several decades, C is approximately a stretched exponential in $t - t_w$, but (see the inset) at short time a power-law behavior is found (dashed line) on several time decades.

$C(t, t_w)/C_\infty$ for several different values of N_{ext} as a function of the scaling variable $(t - t_w)/\tau(N_{ext}, T)$: all the data (for all t_w and N_{ext}) fall on the same master function (which is more general than the above KWW fit).

The pre-asymptotic dynamics (i.e., $t, t_w \ll \tau$) is also of interest and consistent with our previous results: $C(t, t_w)$ has a power-law regime over several decades in time

$$C(t, t_w) \simeq C_0 \left(\frac{t - t_w}{\tau} \right)^{a_c}. \quad (14)$$

The exponent a_c is shown in Fig. 11 as a function of N_{ext} : it is almost constant, $a_c \simeq 1.7$, except at very small or high fields. Note that the τ in Eq. (14) is the same as in Eq. (13), but the exponents a_c and β are numerically different (see Figs. 11 and 12).

B. Off-equilibrium relaxation

The present scenario changes for temperatures around and below T_g where strong off-equilibrium behaviors are found.

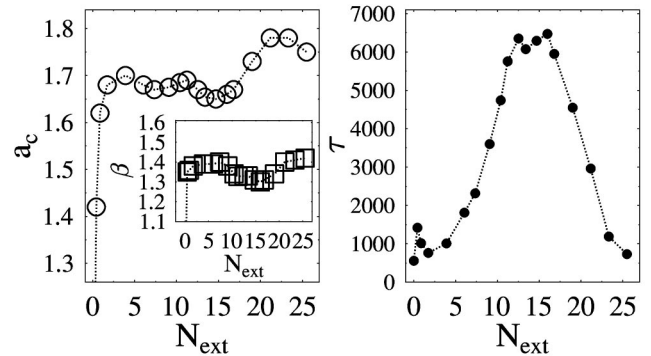


FIG. 11. The exponent a_c of the short-time power-law relaxation of $C(t, t_w)$ of Fig. 10 (for $t_w=10^2$), the KWW exponent β , and the characteristic time τ of its long-time stretched exponential decay, are shown as functions of the applied field N_{ext} .

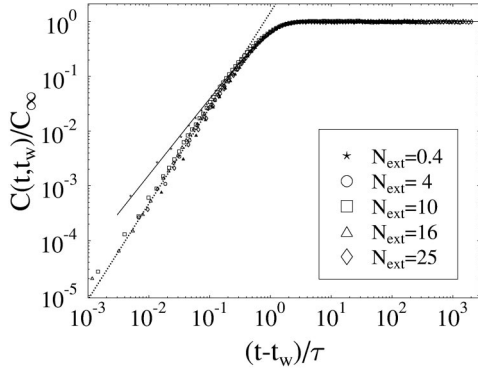


FIG. 12. The two-time correlation function $C(t, t_w)$ in Fig. 10, for the shown values of the external field ($T = 1.0$), are all collapsed on the same master function when plotted as a function of $(t - t_w)/\tau$, where τ is the characteristic relaxation time. This shows that at equilibrium no “aging” is present in C . The bold continuous line is a fit with the KWW function of the asymptotic region, and the dotted line is the initial region power-law fit.

We investigate in this section the dynamics of a system below T_g . We have already seen that for $T < T_g$ relaxation still takes place, though its nature is very different from the relaxation for $T > T_g$. For $T < T_g$ the systems clearly exhibit aging. This phenomenon, typical of off equilibrium dynamics, occur in many different systems ranging from polymers,²² to supercooled liquids,^{19,22} spin glasses,^{21,22} or granular media.⁵⁵ The origin of aging and its apparent universality are important theoretical questions broadly studied in recent years.^{21,56–58}

Figure 13 clearly shows that $C(t, t_w)$ at $T = 0.1$ ($\kappa^* = 0.28$) exhibits strong aging, in the sense that $C(t, t_w)$ explicitly depends on both times t and t_w and not only on the relative time distance $t - t_w$. This is in contrast to the situations close to equilibrium, where C is a function only of $t - t_w$. Here the behavior of C explicitly depends on the wait-

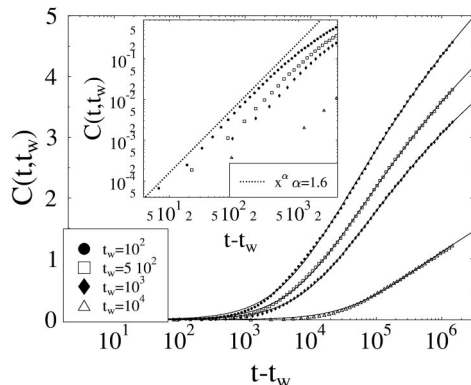


FIG. 13. Logarithmic time relaxation of the two-time vortex-density correlation function $C(t, t_w)$, in the ROM, recorded for $N_{ext} = 16$ ($\kappa^* = 0.28$). $C(t, t_w)$ shows strong “aging” and “stiffening” with t_w . The superimposed lines are the log fits of the text. Inset: the same data of the main frame plotted on log-log scale to show the short-time power-law deviations from logarithmic behavior.

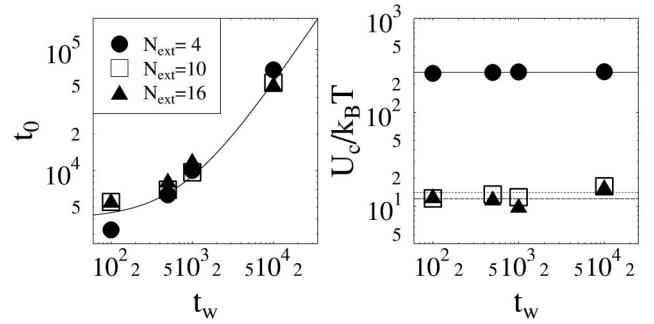


FIG. 14. The parameters of the asymptotic logarithmic fit of the two-time correlation function $C(t, t_w)$ of Fig. 13 as a function of the waiting time t_w . U_c is numerically independent of N_{ext} in the considered broad range, and t_0 is a linear function of t_w (the continuous line is a linear fit).

ing time, t_w , elapsed since the system preparation. Note that an interesting phenomenon is observed: the system relaxation is slower the longer is its “age” t_w . Such a dynamical “stiffening” is also typical of glass formers.^{19,22}

It is important to stress that analysis limited to slowly relaxing “one-time” quantities, such as $M(t)$, may lead to the misleading impression that the system is nearly at stationarity and close to equilibrium. The analysis of $C(t, t_w)$ points out that this is not the case. This is an important observation in order to avoid wrong extrapolations from equilibrium properties.²¹

Let us discuss now in detail the times dependence of $C(t, t_w)$ in the low- T region. Here, where equilibration times are very long, $C(t, t_w)$, after the initial power-law behavior, is well fitted by a generalization of the known logarithmic interpolation formula, often experimentally used¹. For the fit to be successful one need to introduce the *waiting time* t_w explicitly into the formula:

$$C(t, t_w) \simeq C_\infty \left\{ 1 - \left[1 + \frac{\mu T}{U_c} \ln \left(\frac{t + t_0}{t_w + t_0} \right) \right]^{-1/\mu} \right\}. \quad (15)$$

As for $M(t)$, we found that to take $\mu \approx 1$ is consistent with our data. In the above fit $U_c/\mu T$ only depends on N_{ext} and, interestingly, t_0 is approximately a linear function of t_w : $t_0 \propto t_w + t_0^*$, where t_0^* is a constant (see Fig. 14).

More than the three parameters fit in itself, the interest is in the presence of *scaling properties* of purely dynamical origin in the off-equilibrium relaxation. This is shown in Fig. 15, where data for different fields N_{ext} and different waiting times t_w are rescaled to collapse onto a single scaling function. The above results imply that for large enough times, though smaller than the equilibration time, $C(t, t_w)$ is a universal function of the ratio t/t_w : $C(t, t_w) \sim \mathcal{S}(t/t_w)$.

This scaling behavior is in agreement with general scaling properties in off equilibrium dynamics (see Ref. 57) and close analogies appear with other glass formers.^{19,21,22,55,57} In particular, the above scaling form [$C(t, t_w) \sim \mathcal{S}(t/t_w)$, in which $C(t, t_w)$ is a function only of the ratio t/t_w], in glassy system is usually called “simple aging.”²¹ Experimental measurements of $C(t, t_w)$ do not exist yet, but would be extremely important for the identification of the true nature of

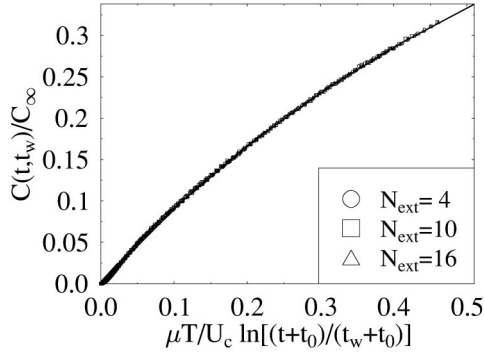


FIG. 15. Off-equilibrium dynamical scaling. Superimposed on the same master function are relaxation data of $C(t, t_w)$ recorded for $N_{ext}=4, 10$, and 16 ($\kappa^*=0.28$, and $T=0.1$) for each $t_w=10^2, 5 \times 10^2, 10^3$, and 10^4 . The asymptotic dynamical scaling is $C(t, t_w) \sim S(t/t_w)$.

dynamical phenomena of vortices in superconductors. The presence of “aging” in magnetic relaxation, $M(t)$, was recently observed in Ref. 14.

V. MEAN-SQUARE DISPLACEMENT AND SELF-SCATTERING FUNCTION

The magnetization dynamics described above can be analyzed in further depth by considering microscopic quantities associated with vortex motions, such as their mean-square displacement or the self scattering function. Below we discuss these quantities. The mean-square displacement is defined as

$$R^2(t) = \frac{1}{N} \left\langle \sum_i [\vec{r}_i(t) - \vec{r}_i(0)]^2 \right\rangle, \quad (16)$$

where N is the total number of particles present on the lattice and $\vec{r}_i(t)$ is the location of vortex i at time t . The incoherent intermediate scattering function is, by definition,

$$F_q(t, t_w) = \frac{1}{N} \left\langle \sum_j e^{i\vec{q} \cdot \vec{r}_j(t)} e^{-i\vec{q} \cdot \vec{r}_j(t_w)} \right\rangle, \quad (17)$$

where the components of \vec{q} are equal to $2\pi n/L$ with $n \in \{0, \dots, L-1\}$ (the data shown below are for $\vec{q} \parallel y$ and $|q| = 8\pi/L$). In typical liquids, the function F_q can be directly measured in neutron- and light-scattering experiments. F_q is also very important for a theoretical description of dynamical processes in complex fluids.⁵⁹

Usually, vortex relaxation also includes pair creation-annihilation processes. These are, however, highly suppressed at low temperatures or high fields, and vortices can be approximately viewed as moving “particles.” Thus we recorded $R^2(t)$ and $F_q(t, t_w)$ in a specific type of computer simulations where, after ramping the field from zero to N_{ext} at a given rate γ (below $\gamma = 5 \times 10^{-4}$), we let the system evolve subject to the “freezing” of the vortex-antivortex creation-annihilation mechanisms. In order to simulate $R^2(t)$ and $F_q(t, t_w)$ at a definite average density, we eliminate the

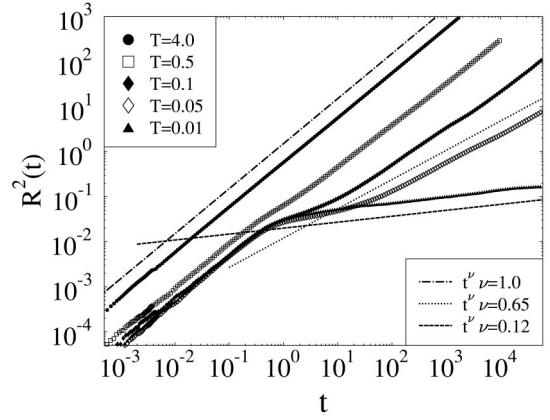


FIG. 16. The vortex mean-square displacement $R^2(t)$ at $N_{ext}=10$ for several temperatures. Below $T_g \sim 0.25$, $R^2(t)$ is strongly subdiffusive: $R^2(t) \sim t^\nu$ with $\nu < 1$. Straight lines are guides for the eye.

reservoir closing the system, and let the vortices move around subject to periodic boundary conditions. We stress that the above approximation of the “real” dynamics is only reasonable at high fields and low temperatures where creation-annihilation is practically absent. Within this kind of dynamics, one can (at the coarse-grained level) define the particle positions at each time step during the evolution, and record the internal rearrangement of the system. To be able to compare results for different particle densities, in this set of simulations we define one time unit to correspond to an average update of each particle present.

The vortex mean square displacement $R^2(t)$, recorded for $N_{ext}=10$, is shown in Fig. 16 for several temperatures. Well above T_g , $R^2(t)$ is asymptotically linear in t . This fact is consistent with low-density measurements⁴³ and simulations.⁴⁵ Thus we can write that

$$R^2(t) = Dt^\nu, \quad (18)$$

where $D = D(T, N_{ext})$ is the diffusion coefficient and the exponent $\nu(T, N_{ext})$ is simply $\nu = 1$. By lowering T , $R^2(t)$ is still linear in t for both small times and large times, but an inflection region appears at intermediate scales. Thus we distinguish a short-time behavior $R^2(t) \approx D_0 t^{\nu_0}$ and a long-time one $R^2(t) \approx D_\infty t^{\nu_\infty}$. The generalized diffusion coefficients $D_0(T, N_{ext})$ and $D_\infty(T, N_{ext})$ are plotted as a function of N_{ext} in Fig. 17 (for $T=1$) and as a function of T in Fig. 18 (for $N_{ext}=10$). Their behavior is consistent with the one recorded for characteristic equilibration time, τ , defined in Eq. (13).

While the short-time relaxation is always diffusive, i.e., $\nu_0 = 1$, eventually, as is apparent in Fig. 16, for temperatures below T_g , the process at long times becomes strongly subdiffusive, i.e., $\nu_\infty < 1$. The asymptotic exponent ν_∞ crucially depends on T , as shown in Fig. 18, and seems to be approximately constant with N_{ext} .

From this point of view, T_g is related to a sort of structural arrest, where particle displacement, for $T \leq T_g$, becomes dramatically suppressed. Each vortex can rattle inside cages of other neighboring vortices for long times, but its diffusion on long length scales is highly inhibited. The system dynamics

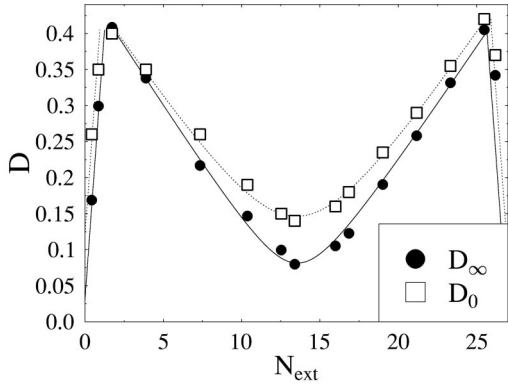


FIG. 17. The diffusion coefficient of vortex motion in the ROM as a function of the external field. D_0 and D_∞ correspond to the short times and asymptotic behaviors. The data shown here are for $T=1.0$, where $R^2(t) \propto t$ (see Fig. 16).

need large-scale “cooperative rearrangements” to relax, in analogy, for instance, with supercooled fluids.¹⁹

Interestingly, a very similar scenario has been recorded in real superconducting samples: for instance, in Ref. 15, it was clearly shown that vortices possess a certain degree of mobility in the low-temperature phase, and only “freeze” below a characteristic field-dependent temperature.

In Fig. 19, we plot the self-scattering function $F_q(t, t_w)$ as a function of $t - t_w$, recorded for $N_{ext}=10$ (similar results are found for other N_{ext}). When $T > T_g$, $F_q(t, t_w)$ shows a KWW relaxation at long times [very similar to the one of Eq. (13), where, for $T=1$, $\beta \approx 0.85$]. $F_q(t, t_w)$ is time translation invariant, i.e., it depends on $t - t_w$, but its KWW behavior gives important information concerning the nature of the microscopic vortex motion: it outlines that the overall vortex diffusion is a non-Gaussian process. In fact, for a Gaussian process we should have found that $\ln F_q(t, 0) \propto -q^2 R^2(t)$. This is clearly not the case here, since $R^2(t) \propto t$ at $T=1$, while $\ln F_q(t, 0) \propto -t^\beta$ with $\beta < 1$.

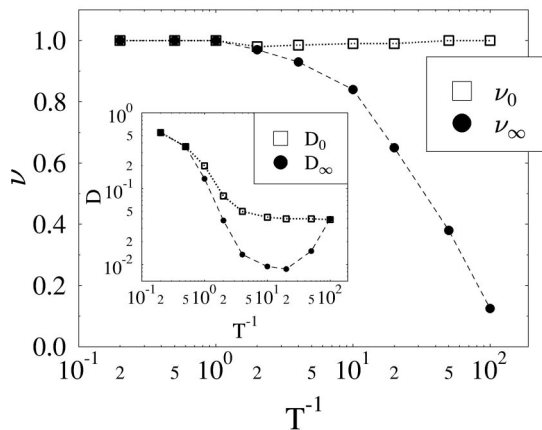


FIG. 18. The short-times (asymptotic) diffusion exponent ν_0 (ν_∞) and coefficient D_0 (D_∞) of the mean-square displacement, $R^2(t) \approx Dt^\nu$, as a function of the temperature ($N_{ext}=10$). Below $T_g \approx 0.25$ the asymptotic dynamics is strongly subdiffusive ($\nu_\infty \ll 1$).

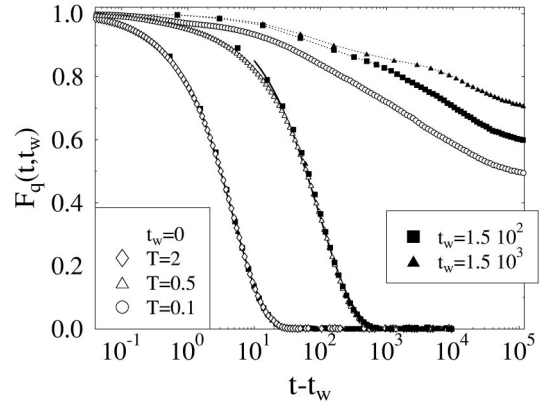


FIG. 19. The self-scattering function $F_q(t, t_w)$ is plotted as a function of $t - t_w$ (here $N_{ext}=10$). The empty symbols are data corresponding to $t_w=0$ for the shown temperatures. The filled symbols are data for $t_w=1.5 \times 10^2$ and 1.5×10^3 (empty squares and triangles). At high temperatures, for instance at $T=2$, $F_q(t, t_w)$ is a function of $t - t_w$, because filled and empty symbols are one on top of the others. At low T , this is no longer the case, and “aging” is seen, as it is apparent for the data with $T=0.1$. The curves superimposed on the data for $T=2$ and 0.5 are stretched exponential asymptotic fits. This outlines that the relaxation process is non-Gaussian (where a simple exponential relaxation should take place). For $T < T_g$, slow logarithmic decay is seen, as shown by the data at $T=0.1$.

At lower temperatures, below T_g , $F_q(t, t_w)$ is also aging, as shown in Fig. 19. It is possible to see that $F_q(t, t_w)$ is not a function of $t - t_w$, because the curves for different t_w do not collapse one on top of the other. Moreover, the time dependence of $F_q(t, t_w)$ is no longer of KWW type, but is asymptotically logarithmically slow, similar to the behavior of the correlation function $C(t, t_w)$ discussed above. The function F_q can be experimentally accessible.

VI. CONCLUSIONS

Summarizing, we studied a model consisting of a coarse-grained version, on a scale l_0 , of a vortex system described by Ginzburg-Landau equations in the London approximation. Such a model was previously shown to have many correspondences to the properties of vortices in superconductors, such as a reentrant phase diagram, magnetization loops with a “second peak” (with a location dependent on the sweep rate of the applied field), properties of Bean profiles, logarithmic creep, “aging” phenomena, nonlinear and history-dependent I - V characteristics, a peak effect in the critical currents, and others.²⁰

In the case considered here, $l_0 \sim \lambda$, the model is schematic but fully tractable, and thus provides a simple description of important mechanisms underlying the complex dynamics of vortex matter. Its equilibrium phase diagram was studied elsewhere:²⁰ our numerical simulations show a sequence of phase transitions; for instance, at low T , when the field is increased two reentrant discontinuous transitions are found and, between them, another discontinuous transition associated to the location of the second magnetization peak.

Here, in particular, we have focused on the details of the dynamics of the magnetization. The system is characterized by relaxation times which depend on the applied field N_{ext} and temperature T : $\tau(N_{ext}, T)$. For a given T , τ is a non-monotonic function of N_{ext} , with a broad maximum around the second peak location. This explains why around the second peak “slushy” regions have been often observed (see, for instance, Refs. 30 and 32): since τ is very large around the second peak, off-equilibrium “glassy” features appear whenever the system is observed on time scales too short compared to τ .

For a given N_{ext} , τ is also a nontrivial function of T and, in particular, increases dramatically when the temperature is lowered (similar to the Vogel-Tamman-Fulcher behavior of glass formers). In fact, below a crossover temperature $T_g(N_{ext})$, it becomes impossible to equilibrate the system on the observation time scales. Above T_g , the magnetic creep shows power laws followed asymptotically by a stretched exponential saturation. In contrast, at very low temperatures, vortex motion is highly suppressed, but not completely absent, and logarithmic creep is recorded. These properties also seem to be found in many experiments,^{1–11,16,23–25} where for instance definite crossover from power-law to logarithmic creep has been observed.

Interestingly, the crossover temperature T_g corresponds to a change in microscopic vortex motion: from diffusive (above T_g) to strongly subdiffusive below T_g .²⁰ However, the analysis of the self-scattering function, $F_q(t, t_w)$, shows that even above T_g vortex diffusion is a non-Gaussian process, and the system dynamics is nontrivial.

In typical experiments or computer simulations, magnetic properties are observed after a zero-field cooling followed by ramping the external field at a given rate γ . Whenever γ is

much larger than the inverse of the characteristic relaxation time, $\tau(N_{ext}, T)$, the system is driven off equilibrium, simply because it is unable to follow the drive, and “memory” and “aging” effects, along with dependences on the field sweep rate, occur.

We showed that, around or below T_g , our system exhibits aging with a definite “dynamical scaling” structure, where two times magnetization correlation functions are of the form: $C(t, t_w) \simeq \mathcal{S}(t/t_w)$. This scenario closely resembles the so called “simple aging” of glassy systems.²¹ In particular, we found that the scaling function \mathcal{S} is well described by a generalization of the “interpolation” formula known for thermal logarithmic creep.

The rapid growth of τ *à la* Vogel, Tamman, and Fulcher, by decreasing the temperature, the very existence of T_g , the slow off equilibrium relaxations, and the sweep rate dependences: all these facts outline a general correspondence between the dynamics of vortices and other glassy systems such as glass formers and supercooled liquids.^{19,21,22} Interestingly, the scenario depicted here is supported by a few available molecular-dynamics simulations of over-damped London-Langevin models,^{20,29} and has many correspondences with experimental findings. Experimental studies of quantities such as $\tau(N_{ext}, T)$ and checks of the scaling properties of $C(t, t_w) \simeq \mathcal{S}(t/t_w)$, as well as $F_q(t, t_w)$ would be of great importance for clarifying the nature of dynamical processes in vortex matter and the relationship between vortex dynamics and the dynamics observed in other glassy systems.

ACKNOWLEDGMENTS

H.J.J. was supported by the EPSRC. M.N. acknowledges support from INFM-PRA(HOP) and INFM-PCI.

*Email address: m.nicodemi@ic.ac.uk

†Email address: h.jensen@ic.ac.uk

¹G. Blatter, M.V. Feigel'man, V.B. Geshkenbein, A.I. Larkin, and V.M. Vinokur, Rev. Mod. Phys. **66**, 1125 (1994).

²E.H. Brandt, Rep. Prog. Phys. **58**, 1465 (1995).

³Y. Yeshurun, A.P. Malozemoff, and A. Shaulov, Rev. Mod. Phys. **68**, 911 (1996).

⁴L.F. Cohen and H.J. Jensen, Rep. Prog. Phys. **60**, 1581 (1997).

⁵K. Ghosh, S. Ramakrishnan, A.K. Grover, Gautam I. Menon, Girish Chandra, T.V. Chandrasekhar Rao, G. Ravikumar, P.K. Mishra, V.C. Sahni, C.V. Tomy, G. Balakrishnan, D. Mck Paul, and S. Bhattacharya, Phys. Rev. Lett. **76**, 4600 (1996); S.S. Banerjee, S. Ramakrishnan, D. Pal, S. Sarkar, A.K. Grover, G. Ravikumar, P.K. Mishra, T.V. Chandrasekhar Rao, V.C. Sahni, C.V. Tomy, M.J. Higgins, and S. Bhattacharya, J. Phys. Soc. Jpn. Suppl. **69**, 262 (2000).

⁶D. Giller, A. Shaulov, R. Prozorov, Y. Abulafia, Y. Wolfus, L. Burlachkov, Y. Yeshurun, E. Zeldov, V.M. Vinokur, J.L. Peng, and R.L. Greene, Phys. Rev. Lett. **79**, 2542 (1997); D. Giller, A. Shaulov, Y. Yeshurun, and J. Giapintzakis, Phys. Rev. B **60**, 106 (1999); M. Baziljevich, D. Giller, M. McElfresh, Y. Abulafia, Y. Radzyner, J. Schneck, T.H. Johansen, and Y. Yeshurun, *ibid.* **62**, 4058 (2000).

⁷Y. Radzyner, S.B. Roy, D. Giller, Y. Wolfus, S. Shaulov, P. Chad-

dah, and Y. Yeshurun, Phys. Rev. B **61**, 14 362 (2000).

⁸L.F. Cohen *et al.*, Physica C **230**, 1 (1994); S.B. Roy, Sajeet Chaudhary, P. Chaddah, and L.F. Cohen, *ibid.* **322**, 115 (1999); G.K. Perkins, L.F. Cohen, A.A. Zhukov, and A.D. Caplin, Phys. Rev. B **51**, 8513 (1995).

⁹S.B. Roy and P. Chaddah, J. Phys.: Condens. Matter **9**, L625 (1997); G. Ravikumar, V.C. Sahni, P.K. Mishra, T.V. Chandrasekhar Rao, S.S. Banerjee, A.K. Grover, S. Ramakrishnan, S. Bhattacharya, M.J. Higgins, E. Yamamoto, Y. Haga, M. Hedo, Y. Inada, and Y. Onuki, Phys. Rev. B **57**, R11 069 (1998); S.S. Banerjee, N.G. Patil, S. Saha, S. Ramakrishnan, A.K. Grover, S. Bhattacharya, M.J. Higgins, E. Yamamoto, Y. Haga, M. Hedo, Y. Inada, and Y. Onuki, *ibid.* **58**, 995 (1998).

¹⁰S. Kokkaliaris, P.A.J. de Groot, S.N. Gordeev, A.A. Zhukov, R. Gagnon, and L. Taillefer, Phys. Rev. Lett. **82**, 5116 (1999).

¹¹Y. Paltiel, E. Zeldov, Y.N. Myasoedov, H. Shtrikman, S. Bhattacharya, M.J. Higgins, Z.L. Xiao, E.Y. Andrei, P.L. Gammel, and D.J. Bishop, Nature (London) **403**, 398 (2000).

¹²S.O. Valenzuela and V. Bekeris, Phys. Rev. Lett. **84**, 4200 (2000).

¹³M. Calame, S.E. Korshunov, Ch. Leemann, and P. Martinoli, Phys. Rev. Lett. **86**, 3630 (2001).

¹⁴E.L. Papadopoulou, P. Nordblad, P. Svedlindh, R. Schöneberger, and R. Gross, Phys. Rev. Lett. **82**, 173 (1999).

¹⁵D.T. Fuchs, E. Zeldov, T. Tamegai, S. Ooi, M. Rappaport, and H.

- Shtrikman, Phys. Rev. Lett. **80**, 4971 (1998).
- ¹⁶S. Bhattacharya and M.J. Higgins, Phys. Rev. Lett. **70**, 2617 (1993); Phys. Rev. B **52**, 64 (1995); W. Henderson, E.Y. Andrei, M.J. Higgins, and S. Bhattacharya, Phys. Rev. Lett. **77**, 2077 (1996); W. Henderson, E.Y. Andrei, and M.J. Higgins, *ibid.* **81**, 2352 (1998).
- ¹⁷Z.L. Xiao, E.Y. Andrei, and M.J. Higgins, Phys. Rev. Lett. **83**, 1664 (1999); Z.L. Xiao, E.Y. Andrei, P. Shuk, and M. Greenblatt, *ibid.* **85**, 3265 (2000).
- ¹⁸M.P.A. Fisher, Phys. Rev. Lett. **62**, 1415 (1989).
- ¹⁹C.A. Angell, Science **267**, 1924 (1995); M.D. Ediger, C.A. Angell, and S.R. Nagel, J. Phys. Chem. **100**, 13 200 (1996).
- ²⁰M. Nicodemi and H.J. Jensen, Phys. Rev. Lett. **86**, 4378 (2001); J. Phys. A **34**, L11 (2001); **34**, 8425 (2001); H.J. Jensen and M. Nicodemi, Europhys. Lett. **54**, 566 (2001); Physica C **341**, 1065 (2000); D.K. Jackson, M. Nicodemi, G. Perkins, N.A. Lindop, and H.J. Jensen, Europhys. Lett. **52**, 210 (2000); M. Nicodemi and H.J. Jensen, Phys. Rev. Lett. **87**, 259702 (2001); H.J. Jensen and M. Nicodemi, Europhys. Lett. **57**, 348 (2002).
- ²¹J. P. Bouchaud, L. F. Cugliandolo, J. Kurchan, and M. Mezard, in *Spin Glasses and Random Fields*, edited by A. P. Young (World Scientific, Singapore, 1997).
- ²²L. C. E. Struik, in *Physical Aging in Amorphous Polymers and Other Materials* (Elsevier, Amsterdam, 1978); Materials Science and Technology, edited by J. Zarzycki (VHC, Weinheim, 1991).
- ²³Y. Abulafia, A. Shaulov, Y. Wolfus, R. Prozorov, L. Burlachkov, Y. Yeshuru, D. Majer, E. Zeldov, H. Whl, V.B. Geshkenbein, and V.M. Vinokur, Phys. Rev. Lett. **77**, 1596 (1996); Y. Yeshurun, N. Bontemps, L. Burlachkov, and A. Kapitulnik, Phys. Rev. B **49**, 1548 (1994).
- ²⁴H. Kupfer, A.A. Zhukov, A. Will, W. Jahn, R. Meier-Hirmer, Th. Wolf, V.I. Voronkova, M. Klser, and K. Saito, Phys. Rev. B **54**, 644 (1996).
- ²⁵N. Chikumoto, M. Konczykowski, N. Motohira, and A.P. Malozemoff, Phys. Rev. Lett. **69**, 1260 (1992).
- ²⁶See *Spin Glasses and Random Fields*, edited by A. P. Young (World Scientific, Singapore, 1998).
- ²⁷K. Binder, Rep. Prog. Phys. **60**, 487 (1997).
- ²⁸G. Parisi, Phys. Rev. Lett. **79**, 3660 (1997).
- ²⁹C. Reichhardt, A. van Otterlo, and G.T. Zimanyi, Phys. Rev. Lett. **84**, 1994 (2000); C.J. Olson, G.T. Zimanyi, A.B. Kolton, and N. Grönbech-Jensen, *ibid.* **85**, 5416 (2000).
- ³⁰S.S. Banerjee, A.K. Grover, M.J. Higgins, Gutam I. Menon, P.K. Mishra, D. Pal, S. Ramakrishnan, T.V. Chandrasekhar Rao, G. Ravikumar, V.C. Sahni, S. Sarkar, and C.V. Tomy, Physica C **355**, 39 (2001).
- ³¹H.J. Jensen, Phys. Rev. Lett. **64**, 3103 (1990); M. Franz and S. Teitel, Phys. Rev. Lett. **73**, 480 (1994); R.A. Hyman, M. Wallin, M.P.A. Fisher, S.M. Girvin, and A.P. Young, Phys. Rev. B **51**, 15 304 (1995).
- ³²T. Nishizaki and N. Kobayashi, Supercond. Sci. Technol. **13**, 1 (2000).
- ³³M. Niderost, A. Suter, P. Visani, and A.C. Mota, Phys. Rev. B **53**, 9286 (1996).
- ³⁴A. Pollini *et al.*, Physica B **165-166**, 365 (1990); A. Amann, A.C. Mota, M.B. Maple, and H.v. Lohneysen, Phys. Rev. B **57**, 3640 (1998).
- ³⁵R.E. Rudd and J.Q. Broughton, Phys. Rev. B **58**, R5893 (1998); S. Kohlhoff, P. Gumbsch, and H.F. Fischmeister, Philos. Mag. A **64**, 851 (1991); A.G. Bashkurov and D.N. Zubarev, Theor. Math. Phys. **1**, 311 (1969).
- ³⁶W. Barford, Phys. Rev. B **56**, 425 (1997).
- ³⁷K.E. Bassler and M. Paczuski, Phys. Rev. Lett. **81**, 3761 (1998); K.E. Bassler, M. Paczuski, and G.F. Reiter, *ibid.* **83**, 3956 (1999); G. Mohler and D. Stroud, Phys. Rev. B **60**, 9738 (1999); R. Cruz, R. Mulet, and E. Altshuler, Physica A **275**, 15 (2000); K.E. Bassler, M. Paczuski, and E. Altshuler, cond-mat/0009278 (unpublished).
- ³⁸R. Mulet, R. Cruz, and E. Altshuler, cond-mat/9912103 (unpublished).
- ³⁹Here we use $A_0=1.0$ as the energy unit, and set $k_B=1$. The other parameters are $A_0^p=0.3A_0$, $N_{c2}=27$, $p=1/2$, and, if not differently stated, $A_1=0.28A_0$ (the \mathcal{H} parameters can be related to the real material parameters²⁰). $L=32$, but the results are checked up to $L=128$.
- ⁴⁰H.J. Jensen, A. Brass, and A.J. Berlinsky, Phys. Rev. Lett. **60**, 1676 (1988); Phys. Rev. B **38**, 9235 (1988); H.J. Jensen, A. Brass, Y. Brechet, and A.J. Berlinsky, *ibid.* **41**, 6394 (1990).
- ⁴¹F. Nori, Science **271**, 1373 (1996); O. Pla and F. Nori, Phys. Rev. Lett. **67**, 919 (1991); C. Reichardt, C.J. Olson, J. Groth, S. Field, and F. Nori, Phys. Rev. B **52**, 10 441 (1995); C.J. Olson, C. Reichardt and F. Nori, *ibid.* **56**, 6175 (1997); Phys. Rev. Lett. **80**, 2197 (1998); **81**, 3757 (1998).
- ⁴²A.E. Koshelev and V.M. Vinokur, Phys. Rev. Lett. **73**, 3580 (1994).
- ⁴³A.M. Troyanovski, J. Aarts, and P.H. Kes, Nature (London) **399**, 665 (1999).
- ⁴⁴R. Surdeanu, R.J. Wijngaarden, E. Visser, J.M. Huijbregtse, J.H. Rector, B. Dam, and R. Griessen, Phys. Rev. Lett. **83**, 2054 (1999).
- ⁴⁵D. Monier and L. Fructer, Eur. Phys. J. B **17**, 201 (2000).
- ⁴⁶D.R. Nelson, Phys. Rev. Lett. **60**, 1973 (1988).
- ⁴⁷M. Daeumling, J.M. Seuntjens, and D.C. Larbalestier, Nature (London) **346**, 332 (1990); G. Yang, P. Shang, S.D. Sutton, I.P. Jones, J.S. Abell, and C.E. Gough, Phys. Rev. B **48**, 4054 (1993); X.Y. Cai, X.Y. Cai, A. Gurevich, D.C. Larbalestier, R.J. Kelley, M. Onellion, H. Berger, and G. Margaritondo, *ibid.* **50**, 16 774 (1994); A.A. Zhukov, H. Kpfer, G. Perkins, L.F. Cohen, A.D. Caplin, S.A. Klestov, H. Claus, V.I. Voronkova, T. Wolf, and H. Whl, *ibid.* **51**, 12 704 (1995); A.K. Pradhan *et al.*, Physica C **264**, 09 (1996); H. Kupfer, A.A. Zhukov, A. Will, W. Jahn, R. Meier-Hirmer, Th. Wolf, V.I. Voronkova, M. Klser, and K. Saito, Phys. Rev. B **54**, 644 (1996).
- ⁴⁸L. Krusin-Elbaum, L. Civale, V.M. Vinokur, and F. Holtzberg, Phys. Rev. Lett. **69**, 2280 (1992).
- ⁴⁹M. Giura, R. Marcon, E. Silva, and R. Fastampa, Phys. Rev. B **46**, 5753 (1992); S. Sarti, R. Fastampa, M. Giura, E. Silva, and R. Marcon, *ibid.* **52**, 3734 (1995).
- ⁵⁰J.R. Thompson, Y.R. Sun, and F. Holtzberg, Phys. Rev. B **44**, 458 (1991).
- ⁵¹A.C. Mota *et al.*, Phys. Scr. **T45**, 69 (1992).
- ⁵²J.Z. Liu, Lu Zhang, M.D. Lan, R.N. Shelton, and M.J. Fluss, Phys. Rev. B **46**, 9123 (1992).
- ⁵³Y. Xu, M. Suenaga, A.R. Moodenbaugh, and D.O. Welch, Phys. Rev. B **40**, 10 882 (1989).
- ⁵⁴D.A. Brawner, N.P. Ong, and Z.Z. Wang, Phys. Rev. B **47**, 1156 (1993).

- ⁵⁵M. Nicodemi, Phys. Rev. Lett. **82**, 3734 (1999); M. Nicodemi and A. Coniglio, *ibid.* **82**, 916 (1999); M. Nicodemi, Physica A **257**, 448 (1998); **285**, 267 (2000); J. Phys. I **7**, 1365 (1997).
- ⁵⁶M. Mezard and G. Parisi, Phys. Rev. Lett. **82**, 747 (1999).
- ⁵⁷A. Coniglio and M. Nicodemi, Phys. Rev. E **59**, 2812 (1999).
- ⁵⁸W. Kob, *Annual Reviews of Computational Physics*, edited by D. Stauffer (World Scientific, Singapore, 1995), Vol. III, p. 1; M. Nicodemi and A. Coniglio, J. Phys. A **30**, L187 (1997); W. Kob and J.-L. Barrat, Phys. Rev. Lett. **78**, 4581 (1997); G. Parisi, *ibid.* **79**, 3660 (1997).
- ⁵⁹W. Götze, in *Liquids, Freezing and the Glass Transition*, edited by J. P. Hansen, D. Levesque, and J. Zinn-Justin, Les Houches. Session LI, 1989 (North-Holland, Amsterdam, 1991), p. 287; W. Götze and L. Sjögren, Rep. Prog. Phys. **55**, 241 (1992).